JCTC Journal of Chemical Theory and Computation

Article

pubs.acs.org/JCTC

New Insights into the Molecular Mechanism of E-Cadherin-Mediated Cell Adhesion by Free Energy Calculations

Fabio Doro,[†,§] Giorgio Saladino,[‡] Laura Belvisi,[†] Monica Civera,*[,†] and Francesco L. Gervasio*[,‡]

[†]Department of Chemistry, University of Milan, Via Camillo Golgi 19, Milan I-20133, Italy

[‡]Department of Chemistry and Institute of Structural and Molecular Biology, University College London, 20 Gordon Street, London WC1H 0AJ, United Kingdom

Supporting Information

ABSTRACT: Three-dimensional domain swapping is an important mode of protein association leading to the formation of stable dimers. Monomers associating via this mechanism mutually exchange a domain to form a homodimer. Classical cadherins, an increasingly important target for anticancer therapy, use domain swapping to mediate cell adhesion. However, despite its importance, the molecular mechanism of domain swapping is still debated. Here, we study the conformational changes that lead to activation and dimerization via domain swapping of E-cadherin. Using state-of-the-art enhanced sampling atomistic simulations, we reconstruct its conformational free energy landscape, obtaining the free energy profile connecting the inactive and active form. Our simulations predict that the E-cadherin monomer populates the open and closed forms almost equally, which is in agreement with the proposed "selected fit" mechanism in which monomers in an active conformational state bind to form a homodimer, analogous to the conformational selection mechanism often observed in ligand−target binding. Moreover, we find that the open state population is increased in the presence of calcium ions at the extracellular boundary, suggesting their possible role as allosteric activators of the conformational change.

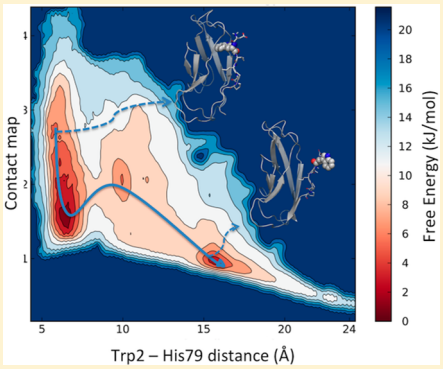

INTRODUCTION

Protein−protein interactions play such a fundamental role in living organisms that proteins are prevalently found in a multimeric aggregation state. Oligomerization can occur in different ways. A common and intriguing mode of association is the so-called three-dimensional (3D) domain swapping[1] in which oligomers are formed from monomers by exchanging domains. The swapping domains, connected to the remaining part of the protein by a portion called the "hinge loop", can either be a single secondary structure element, such as a β-strand, or a more extended, multistructured polypeptide chain. In the monomeric state, the swapping domains are folded inside an acceptor pocket ("closed form"), whereas in the oligomeric form, they extend onto the corresponding pocket of another protein ("open form").[2]

Among proteins exhibiting 3D domain swapping, cadherins are of particular interest. A large family of calcium-dependent adhesion molecules found at intercellular junctions, cadherins mediate cell−cell adhesion by forming dimers between the N-terminal domains of two proteins localized on adjacent cells.[3] Cadherin's pivotal role in cell adhesion explains the involvement of several of these proteins in tumor progression, making them a promising target for anticancer therapies. For instance, E-cadherin, regarded as the prototypical member of classical cadherins, has been reported to play a critical role in the proliferation of various types of cancer.[4,5] For this reason, new anticancer agents targeting cadherins are being developed.[6,7]

Classical cadherins consist of an N-terminal extracellular (EC) portion, constituted by five domains (EC1−EC5) rigidified at the interface by calcium ions. Dimerization occurs through the mutual exchange of a highly conserved N-terminal sequence comprised of the six residues DWVIPP (the "adhesion arm"). In particular, the Trp residue, which in the closed form is inserted in a hydrophobic pocket within EC1 of the same protein, is docked in the corresponding binding site of the partner protein in the swap dimer (Figure 1). Clusterization of such swap dimers at the cellular interface leads to the formation of organized oligomers.[8]

In the past decade, experimental data have suggested the existence of two possible 3D swapping mechanisms; a selected fit and an induced fit pathway (Figure S1, Supporting Information) have been reported.[9−13] The former mechanism assumes that monomers in the closed form first undergo a conformational change leading to the active open form and only in a second step can they bind each other. According to the induced fit mechanism, the dimerization occurs via an intermediate complex, the "encounter complex", that lowers the energy barrier required for swapped dimer formation. The mechanism through which the two monomers form the

Received: November 14, 2014
Published: March 3, 2015

DOI: 10.1021/ct5010164
J. Chem. Theory Comput. 2015, 11, 1354−1359

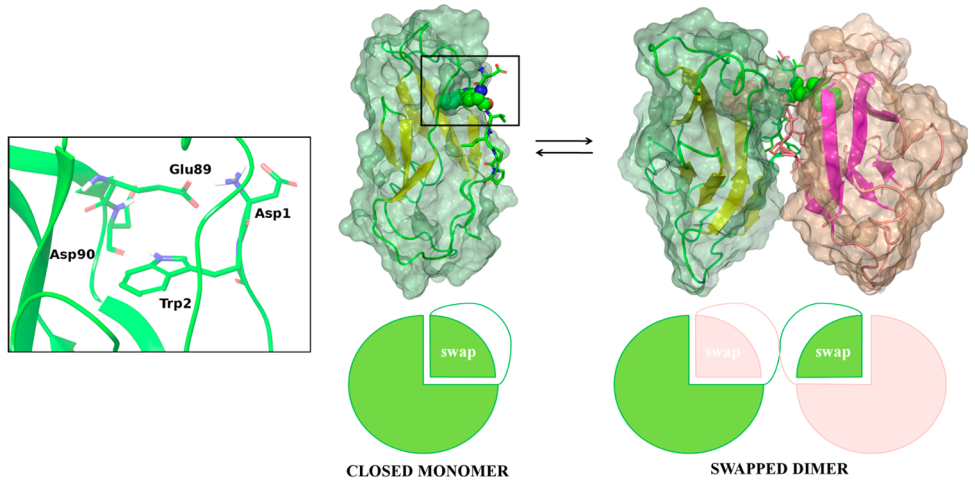

Figure 1. Adhesive binding mechanism of classical cadherins as an example of 3D domain swapping. In the closed form, Trp2 is inserted in its own hydrophobic pocket, whereas in the swapped dimer, it binds to the hydrophobic pocket of another cadherin molecule (PDB ID: 3Q2V). To the left, the salt bridge formed in the closed monomer between the side chain of Glu89 and the N-terminus NH_3^+ of Asp1 can also be appreciated. The structure for the closed monomer is derived from our simulations.

encounter complex, as well as the conformational changes that lead to the swap dimer from the encounter complex, are currently unknown. Moreover, the encounter complex has not yet been structurally characterized, although it is usually associated with the so-called X dimer, an alternative dimer conformation that is formed when swap-impaired cadherins aggregate.[14] However, it is worth noting that mutations that prevent the formation of the X dimer do not alter the ability of classical cadherins to form swap dimers.[12] This suggests the existence of at least two alternative mechanisms of dimerization of classical cadherins. Herein, we investigate the selected fit hypothesis by reconstructing the free energy profile of the conformational transition of the type I E-cadherin monomer from its closed inactive state to its open form. This represents the first step of the supposed two-step selected fit mechanism. Only if the free energy and population of the two forms are comparable could a selected fit mechanism be possible.

The time scale involved in the swapping mechanism prevents the observation of conformational changes in cadherins with conventional molecular dynamics (MD) simulations. For this reason, we used a state-of-the-art enhanced sampling technique, namely, a combination of parallel tempering and metadynamics (PT-MetaD).[15]

This method has been successfully used to converge the multidimensional free energy landscape associated with the folding of small proteins,[15,16] complex conformational changes in protein kinases,[17,18] and the folding and oligomerization of fibritin foldon domains.[19] In the well tempered ensemble (WTE) methodology used in the present study, a static bias on the potential energy of the system is applied in the PT-MetaD simulation with the purpose of increasing the energy overlap between replicas and thus enhancing the sampling efficacy.[20]

Because calcium ions modulate cadherin's biological activity, we also investigated their role in the E-cadherin monomer closed-to-open transition. First, we assessed the stability of the EC1-EC2 domain with and without calcium ions by performing two 100 ns unbiased MD simulations (Figure S2, Supporting Information). As also shown in a previous study,[21] the absence of Ca^{2+} ions at the EC boundary causes the system to lose its linearity, which is needed by cadherin to carry out its functions. As a consequence, the systems for the subsequent biased simulations were set up as follows: (1) EC1 domain with no Ca^{2+} ions and (2) EC1-EC2 domain containing three Ca^{2+} ions at the interdomain boundary. By analyzing the free energy profiles of the two systems, we extrapolated the impact of the calcium ions in favoring the E-cadherin conformational change.

EXPERIMENTAL SECTION

In a recent comparative study,[22] CHARMM22*[23] and Amber99SB*-ILDN[23,24] were ranked among the best protein force fields with both reproducing a wide range of experimental data. More recently, we compared the performance of these two force-fields together with PT-metaD in reproducing the conformational energy landscape of proline isomerase.[25] Both were able to reproduce the experimental free energy difference between the major and minor conformers, but the simulations performed with CHARMM22* showed enhanced flexibility in agreement with previous observations that it might be better at predicting the folding kinetics of small proteins. Thus, we performed our simulations here using the CHARMM22* force field together with GROMACS 4.5.5[26] and PLUMED 1.3.[27] We obtained the initial coordinates from the X-ray structure (PDB ID: 1FF5)[28] of an E-cadherin X dimer, which is the only available experimental structure in a closed conformation. Then, we constructed two independent monomeric systems in the closed form: EC1 containing residues 1−99 and no calcium ions, and EC1-EC2 containing residues 1−215, three Ca^{2+} ions at the extracellular boundary, and a fourth calcium ion at the end of EC2. The first system was solvated in a rhombic dodecahedron box with 9253 TIP3P water molecules, and the second was solvated in a triclinic box with 15136 TIP3P water molecules. Calcium ions were modeled following the method of Bjelkmar and co-workers.[29,30] We started our simulations by first minimizing the systems using a steepest descent algorithm.[30] We then performed an equilibration in two steps: First, we simulated the systems for 1 ns at 300 K in an NVT ensemble using the velocity-rescale thermostat[31] and positional restraint on the proteins. Then, we performed a 10 ns NPT simulation using a Parrinello−Rahman barostat[32] with no restraint to conclude the equilibration. The particle mesh Ewald method was used for treating long-range electrostatics

DOI: 10.1021/ct5010164
J. Chem. Theory Comput. 2015, 11, 1354−1359

using a cutoff of 10 Å. A time step of 2 fs was used for all simulations.

To be able to run in the WTE, we first performed a preliminary PT-MetaD[15,16] run with four replicas of each system using the potential energy as the only collective variable (CV), according to the original WTE article.[20] Temperatures for each replica were 300, 330, 362, and 398 K. Gaussians with a height of 4.0 kJ/mol were added every 500 MD steps. Exchanges among replicas were attempted every 250 MD steps. The average exchange probability was ∼30% for both systems. The obtained bias on the potential energy was kept fixed during the following PT-MetaD run, thus running in the WTE ensemble.

The production run for each system was performed using the following three collective variables: the distance between His79 Cα and the centroid of the indole moiety in Trp2 (CV1), which is needed to discriminate between closed and open conformations, the improper dihedral defined by two heavy atoms in the Trp indole ring and the centroids of two sets of Cα atoms in β-strand regions 73−80 and 92−97 (CV2), which describes the orientation of Trp2 indole moiety inside the cavity well, and a contact map counting the number of selected contacts between the adhesion arm and its pocket (CV3). The contact map was selected on the basis of the cluster analysis of snapshots of closed, intermediate, and open forms of E-cadherin taken from short MetaD simulations. Analysis of the different atom distances between the hydrophobic pocket and the opening arm, in the three forms, allowed us to define a CV describing the path along which the conformational change occurs (see Figure S3 and Table S1, Supporting Information, for a depiction of the CVs). Gaussians 1.3 kJ/mol in height were added every 500 MD steps using a bias factor of 12 for both systems. Simulations were run in NVT conditions with a time step of 2 fs until all of the interesting regions in the CV space were fully explored. To assess the convergence of the simulations, we applied a recently developed reweighting algorithm by Tiwary and Parrinello[33] and obtained a time-independent estimate of the free energy (see Figure S4, Supporting Information, for projection of the free energy onto CV1) from which we calculated the error of the free energy differences. In addition, we independently reran the EC1 system and verified that the reconstructed free energies converge to the same profile (Figure S5, Supporting Information).

Conformations belonging to each minimum were extracted and clustered using the g_cluster GROMACS tool with a single linkage method and a cutoff of 1 Å over the RMS distance computed on EC1 Cα atoms.

RESULTS

The conformational free energy surfaces projected onto two relevant coordinates, the His79−Trp2 distance (CV1) and the orientation of the Trp2 indole moiety with respect to the protein backbone (CV2), are shown in Figure 2.

In both systems, the global minimum corresponds to a closed conformation (minimum A in both maps) with the Trp2 side chain being firmly docked into its hydrophobic pocket and forming a hydrogen bond with the Asp90 backbone, as observed in the X-ray structure. However, whereas the EC1-EC2 complex is characterized by a salt bridge between the Asp1 N-terminus and the Glu89 side chain (99% of the structures), EC1 alone formed this interaction in only 47% of the structures (in the remaining 53%, the Asp1 N-terminus is exposed to the solvent). Only at higher energies (at least 8 kJ/mol) could we observe closed conformations in which the indole moiety plane is oriented differently inside the pocket, pointing either toward Glu89 (90 deg rotation of the indole plane with respect to the structures representing the global minimum) or Lys25 (180 deg rotation). These conformations, characterized by a loose Asp1−Glu89 salt bridge, are likely to represent metastable closed-like forms with weaker interactions between the adhesion arm and the hydrophobic pocket. These findings regarding the closed form of both systems are in agreement with the hypothesis of an open/closed state equilibrium in which the Trp2 indole exits the cavity and re-enters it at a different orientation.

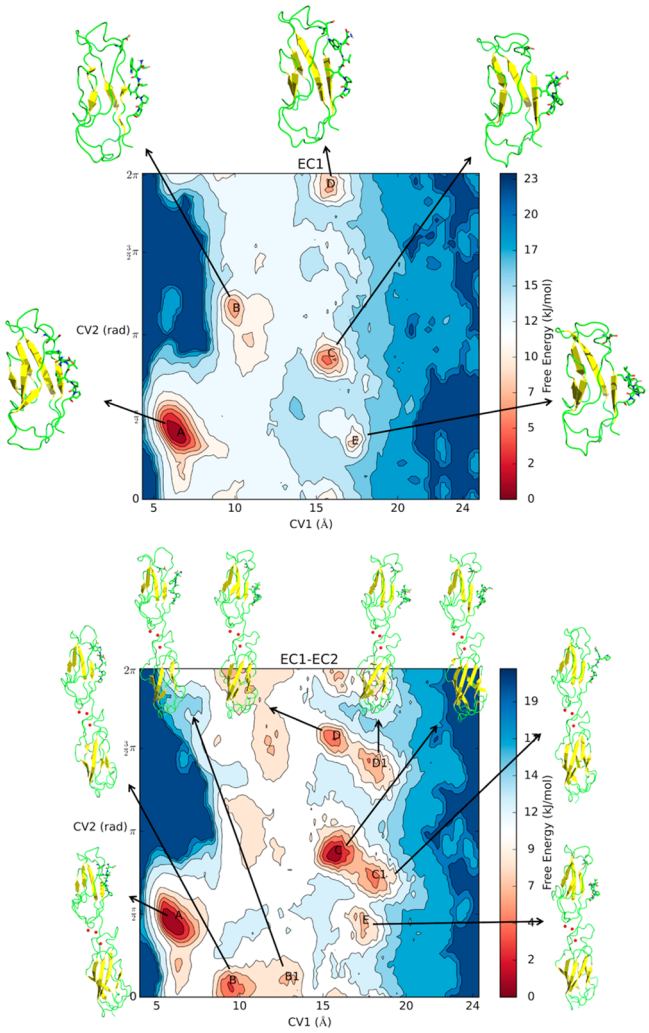

Figure 2. Free energy surfaces associated with the closed-to-open conformational transition of EC1 (top) and EC1-EC2 (bottom) E-cadherin projected on the CV1 (Trp2−His79 distance) and CV2 (Trp2 orientation) space at 300 K. The most representative structures of each local minimum obtained from cluster analysis are reported. Contour lines are drawn with a stride of 2 kJ/mol.

The other energy minima found on the maps represent different open states of EC1 (Figure 2, up) and EC1-EC2 (Figure 2, down). Indeed, the Trp2 side chain is relatively free to move in solution making it free to adopt different conformations. The presence of calcium ions at the EC boundary seems to enhance this entropy-driven process, because in EC1-EC2, we observe a broader selection of open conformations. In both cases, the open forms adopt different positions of the indole Trp2 ring with respect to the protein

DOI: 10.1021/ct5010164
J. Chem. Theory Comput. 2015, 11, 1354−1359

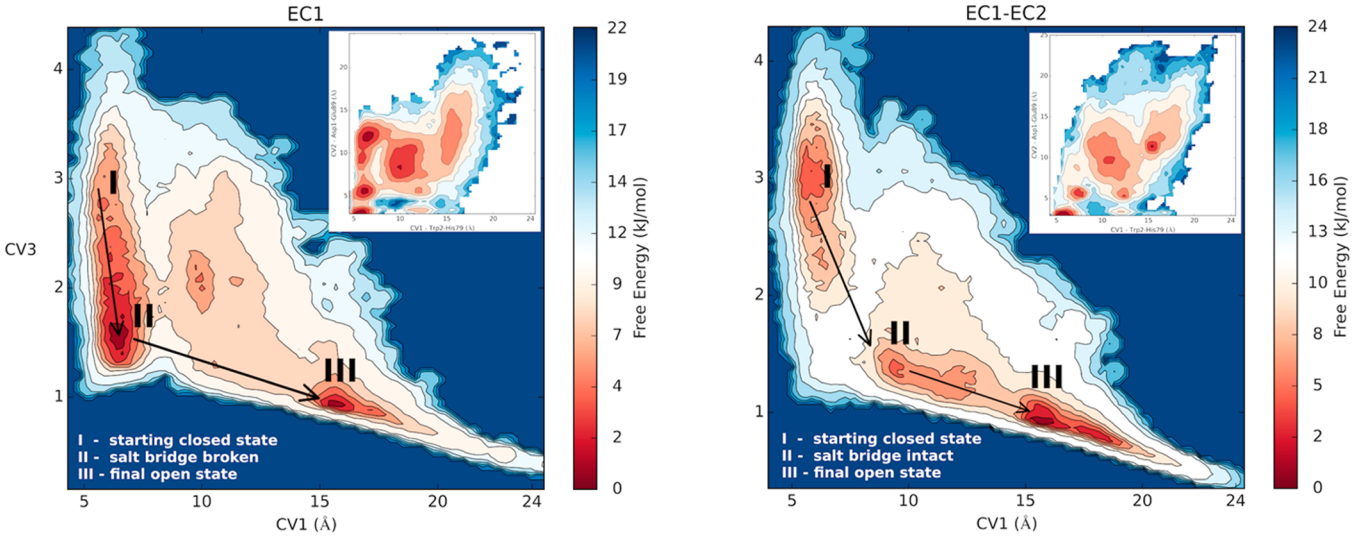

Figure 3. Reconstructed free energies projected on a 2D surface using CV1 and CV3 for EC1 (left) and EC1-EC2 (right) E-cadherin monomers. Isolines are drawn every 2.0 kJ/mol. The salt bridge refers to the electrostatic interaction between Asp1-NH_3^+ and the Glu89 side chain. In EC1, breaking of the salt bridge (I to II) precedes the exit of Trp2 from the pocket (II to III), whereas in EC1-EC2, the indole moiety first leaves the hydrophobic pocket (I to II) and only in a second step does the electrostatic interaction get broken (II to III). We also used a reweighting algorithm to directly project the free energy on the Asp1-NH_3^+−Glu89 salt bridge distance (on the *Y*-axis) and on the Trp2−His79 distance (shown as insets at the top right of each map).

principal axis at the same value of the Trp2 distance from the binding pocket. In fact, considering only the CV1 values (see also Figure S6, Supporting Information), both systems showed two major open states, one located at CV1 values around 10 Å, in which the adhesion arm tends to adhere to the rest of the protein to minimize solvent exposure (Figure 2, minima B), and another that is energetically more favored located at CV1 values around 16 Å in which the adhesion arm is completely exposed to the solvent (Figure 2, minima C, D, and E). It is worth noting that the most representative structures of EC1-EC2 belonging to minimum C1 superimpose to the open conformation of the X-ray swap dimer structure well (PDB ID: 3Q2V,[8] Cα RMSD = 0.76 Å, Figure S7, Supporting Information). In EC1, the energy difference between the main open and closed minima is 5.4 ± 1.5 kJ/mol, whereas in EC1-EC2, the minimum located at 16 Å is isoenergetic (with an estimated sampling error of 0.6 kJ/mol) to the closed form. The energetic barriers for the closed/open transition for the EC1-EC2 and EC1 systems, 14 ± 4 and 16 ± 4 kJ/mol, respectively, are within the sampling error. The larger sampling error on the energy barriers is due to the nature of the PT-metaD approach.[15] The energy values for the closed/open barrier described above can be used to estimate the crossing rate between the two states. Because of the diffusive nature of the dynamics, we could follow the approach of Juraszek and co-workers[34] to estimate a transmission coefficient k of $\sim 10^{-3}$ that corrects for the correlated recrossings at the transition state. This allows us to estimate the rates at 56−1400 ns for EC1 and 25−622 ns for EC1-EC2. At both ends of the predicted range, the kinetics are very fast. The fast interconversion rate between open and closed forms is in agreement with a selected fit mechanism. It is worth noting that Miloushev and co-workers[13] have detected the existence of cadherin 8, a type II cadherin, in the open form in solution through NMR dispersion relaxation techniques.

Projection of the free energy on a 2D map using CV1 and CV3 allows for characterization of the arm opening mechanism. The third collective variable (CV3) maps the atomic contacts between the adhesion arm and the hydrophobic pocket (Table S1, Supporting Information). CV3 values around 3 correspond to the starting, closed conformation, whereas values around 1, in which the adhesion arm is completely exposed to the solvent, correspond to a fully open state.

In Figure 3, we report the free energy surface as a function of CV1 and CV3. From analysis of the structures belonging to each minimum, we found that the two systems followed distinct opening pathways. In EC1 (Figure 3, left), the first step is characterized by disruption of the salt bridge (I to II, CV3 from 3 to 2) with the Trp2 side chain docked into its pocket, and only in the second step does Trp2 leave the hydrophobic pocket and expose the indole moiety to the solvent (II to III, CV3 from 2 to 1). A conformational equilibrium was in fact observed for the closed form of EC1 (Figure 2, minimum A, up), where the two most representative conformations differ only by the presence of the salt bridge. For this system, it seems that the lack of calcium ions facilitates breaking of the salt bridge but not opening of the arm. In EC1-EC2 (Figure 3, right, from I to II), the Trp2 indole moiety first moves toward the solvent while maintaining the salt bridge between the Glu89 side chain and Asp1 (CV3 from 3 to 1.5). At this point, the adhesion arm is still relatively close to the rest of the protein, and only in the second step when the salt bridge is broken is it able to fully open (II to III, CV3 from 1.5 to 1). This pathway is in agreement with what was observed during our simulations. In fact, in the first part of the simulation, the Trp2 side chain exited and re-entered the hydrophobic pocket several times without breaking the salt bridge. Only when the salt bridge is broken do these events become less probable. Moreover, this analysis shows that the major contribution to the interaction energy of the adhesive arm with the pocket seems to be derived from the salt bridge between Asp1 and Glu89, two highly conserved residues in all classical cadherins. The same conclusion regarding the two different pathways can be drawn if one observes the free energies projected directly

DOI: 10.1021/ct5010164
J. Chem. Theory Comput. 2015, 11, 1354−1359

onto the salt bridge distance (Figure 3, insets). To extract an unbiased distribution for the Asp1-NH_3^+−Glu89 distance, we used the reweighting algorithm developed by Bonomi and co-workers.[35] Only in EC1 is there a well-defined minimum of CV values (6−12 Å), corresponding to a closed conformation with a broken salt bridge. Vendome and co-workers postulated that calcium ions could introduce some strain in the adhesive arm, and the release of such strain could be the driving force behind opening of the arm.[36] Our findings are in agreement with such a hypothesis—when calcium ions are present, strain is released first by exposing Trp2 to the solvent followed by full opening of the arm—but also introduce the N-terminus−Glu89 salt bridge as a key interaction in the opening.

CONCLUSIONS

Our simulations predict that the EC1-EC2 E-cadherin monomer, in the presence of calcium ions, significantly populates both the open and closed forms, which are almost iso-energetic. This observation is in agreement with the proposed selected fit mechanism. Although recent studies have suggested an induced fit mechanism for E-cadherin,[11] when we attempted protein−protein docking[37] using both the major and minor states of the EC1-EC2 E-cadherin system, we could not reproduce a viable X-dimer conformation (Table S2, Supporting Information). On the contrary, the low free energy penalty and fast kinetics that we predicted for the system strongly suggest a conformational selection mechanism. Moreover, we are able for the first time to provide detailed characterization of the conformational transition of the E-cadherin monomer that was postulated to exist based on the proposed selected fit mechanism. By using a state-of-the-art enhanced sampling algorithm, we obtained a fully converged multidimensional conformational free energy landscape describing the arm opening transition and intermediate metastable states. These states might provide a starting point for the design of new inhibitors and perhaps lead to anticancer agents, as well as help identify the encounter complex structure, which is a necessary step in order to attempt an atomic resolution description of the alternative induced fit mechanism of cadherin dimerization. Finally, our simulations confirm that calcium ions favor opening of the arm by stabilizing the open form.

ASSOCIATED CONTENT

Supporting Information

Proposed mechanisms of dimerization, trajectory analysis for unbiased simulations, CV1−CV2 description, contact map (CV3) description, free energy profiles projected on CV1 with error estimation, and docking results for EC1-EC2. This material is available free of charge via the Internet at http://pubs.acs.org.

AUTHOR INFORMATION

Corresponding Authors

*E-mail: monica.civera@unimi.it.

*E-mail: f.l.gervasio@ucl.ac.uk.

Present Address

§F.D.: Structural Biology and NMR Laboratory, Department of Biology, University of Copenhagen, Ole Maaløes Vej 5, 2200 Copenhagen N, Denmark.

Notes

The authors declare no competing financial interest.

ACKNOWLEDGMENTS

We acknowledge HPC-Europa2 Programme (Application Number 1024) and MIUR (FIRB RBFR088ITV Project) for financial support. We also thank the University of Milan for a Ph.D. Fellowship for F.D. and CINECA for use of their computing facilities.

REFERENCES

(1) Bennett, M. J.; Schlunegger, M. P.; Eisenberg, D. 3D Domain Swapping: A Mechanism for Oligomer Assembly. *Protein Sci.* **1995**, *4*, 2455−2468.

(2) Gronenborn, A. M. Protein Acrobatics in Pairs—Dimerization via Domain Swapping. *Curr. Opin. Struct. Biol.* **2009**, *19*, 39−49.

(3) Leckband, D.; Sivasankar, S. Cadherin Recognition and Adhesion. *Curr. Opin. Cell Biol.* **2012**, *24*, 620−627.

(4) Berx, G.; van Roy, F. Involvement of Members of the Cadherin Superfamily in Cancer. *Cold Spring Harbor Perspect. Biol.* **2009**, *1*, a003129.

(5) De Santis, G.; Miotti, S.; Mazzi, M.; Canevari, S.; Tomassetti, A. E-Cadherin Directly Contributes to PI3K/AKT Activation by Engaging the PI3K-p85 Regulatory Subunit to Adherens Junctions of Ovarian Carcinoma Cells. *Oncogene* **2009**, *28*, 1206−1217.

(6) Blaschuk, O. W.; Devemy, E. Cadherins as Novel Targets for Anti-Cancer Therapy. *Eur. J. Pharmacol.* **2009**, *625*, 195−198.

(7) Doro, F.; Colombo, C.; Alberti, C.; Arosio, D.; Belvisi, L.; Casagrande, C.; Fanelli, R.; Manzoni, L.; Parisini, E.; Piarulli, U.; Luison, E.; Figini, M.; Tomassetti, A.; Civera, M. Computational Design of Novel Peptidomimetic Inhibitors of Cadherin Homophilic Interactions. *Org. Biomol. Chem.* **2015**, *13*, 2570−2573.

(8) Harrison, O. J.; Jin, X.; Hong, S.; Bahna, F.; Ahlsen, G.; Brasch, J.; Wu, Y.; Vendome, J.; Felsovalyi, K.; Hampton, C. M.; Troyanovsky, R. B.; Ben-Shaul, A.; Frank, J.; Troyanovsky, S. M.; Shapiro, L.; Honig, B.; Sergey, M. The Extracellular Architecture of Adherens Junctions Revealed by Crystal Structures of Type I Cadherins. *Structure* **2011**, *19*, 244−256.

(9) Brasch, J.; Harrison, O. J.; Honig, B.; Shapiro, L. Thinking Outside the Cell: How Cadherins Drive Adhesion. *Trends Cell Biol.* **2012**, *22*, 299−310.

(10) Sivasankar, S.; Zhang, Y.; Nelson, W. J.; Chu, S. Characterizing the Initial Encounter Complex in Cadherin Adhesion. *Structure* **2009**, *17*, 1075−1081.

(11) Li, Y.; Altorelli, N. L.; Bahna, F.; Honig, B.; Shapiro, L.; Palmer, A. G. Mechanism of E-Cadherin Dimerization Probed by NMR Relaxation Dispersion. *Proc. Natl. Acad. Sci. U.S.A.* **2013**, *110*, 16462−16467.

(12) Harrison, O. J.; Bahna, F.; Katsamba, P. S.; Jin, X.; Brasch, J.; Vendome, J.; Ahlsen, G.; Carroll, K. J.; Price, S. R.; Honig, B.; Shapiro, L. Two-Step Adhesive Binding by Classical Cadherins. *Nat. Struct. Mol. Biol.* **2010**, *17*, 348−357.

(13) Miloushev, V. Z.; Bahna, F.; Ciatto, C.; Ahlsen, G.; Honig, B.; Shapiro, L.; Palmer, A. G. Dynamic Properties of a Type II Cadherin Adhesive Domain: Implications for the Mechanism of Strand-Swapping of Classical Cadherins. *Structure* **2008**, *16*, 1195−1205.

(14) Ciatto, C.; Bahna, F.; Zampieri, N.; VanSteenhouse, H. C.; Katsamba, P. S.; Ahlsen, G.; Harrison, O. J.; Brasch, J.; Jin, X.; Posy, S.; Vendome, J.; Ranscht, B.; Jessell, T. M.; Honig, B.; Shapiro, L. T-Cadherin Structures Reveal a Novel Adhesive Binding Mechanism. *Nat. Struct. Mol. Biol.* **2010**, *17*, 339−347.

(15) Bussi, G.; Gervasio, F. L.; Laio, A.; Parrinello, M. Free-Energy Landscape for β Hairpin Folding from Combined Parallel Tempering and Metadynamics. *J. Am. Chem. Soc.* **2006**, *128*, 13435−13441.

(16) Deighan, M.; Bonomi, M.; Pfaendtner, J. Efficient Simulation of Explicitly Solvated Proteins in the Well-Tempered Ensemble. *J. Chem. Theory Comput.* **2012**, *8*, 2189−2192.

(17) Lovera, S.; Sutto, L.; Boubeva, R.; Scapozza, L.; Dölker, N.; Gervasio, F. L. The Different Flexibility of c-Src and c-Abl Kinases Regulates the Accessibility of a Druggable Inactive Conformation. *J. Am. Chem. Soc.* **2012**, *134*, 2496−2499.

DOI: 10.1021/ct5010164
J. Chem. Theory Comput. 2015, 11, 1354−1359

(18) Sutto, L.; Gervasio, F. L. Effects of Oncogenic Mutations on the Conformational Free-Energy Landscape of EGFR Kinase. *Proc. Natl. Acad. Sci. U.S.A.* **2013**, *110*, 10616−10621.
(19) Barducci, A.; Bonomi, M.; Prakash, M. K.; Parrinello, M. Free-Energy Landscape of Protein Oligomerization from Atomistic Simulations. *Proc. Natl. Acad. Sci. U.S.A.* **2013**, *110*, E4708−E4713.
(20) Bonomi, M.; Parrinello, M. Enhanced Sampling in the Well-Tempered Ensemble. *Phys. Rev. Lett.* **2010**, *104*, 190601.
(21) Cailliez, F.; Lavery, R. Cadherin Mechanics and Complexation: The Importance of Calcium Binding. *Biophys. J.* **2005**, *89*, 3895−3903.
(22) Lindorff-Larsen, K.; Maragakis, P.; Piana, S.; Eastwood, M. P.; Dror, R. O.; Shaw, D. E. Systematic Validation of Protein Force Fields against Experimental Data. *PLoS One* **2012**, *7*, e32131.
(23) Piana, S.; Lindorff-Larsen, K.; Shaw, D. E. How Robust Are Protein Folding Simulations with Respect to Force Field Parameterization? *Biophys. J.* **2011**, *100*, L47−L49.
(24) Lindorff-Larsen, K.; Piana, S.; Palmo, K.; Maragakis, P.; Klepeis, J. L.; Dror, R. O.; Shaw, D. E. Improved Side-Chain Torsion Potentials for the Amber ff99SB Protein Force Field. *Proteins* **2010**, *78*, 1950−1958.
(25) Papaleo, E.; Sutto, L.; Gervasio, F. L.; Lindorff-Larsen, K. Conformational Changes and Free Energies in a Proline Isomerase. *J. Chem. Theory Comput.* **2014**, *10*, 4169−4174.
(26) Pronk, S.; Páll, S.; Schulz, R.; Larsson, P.; Bjelkmar, P.; Apostolov, R.; Shirts, M. R.; Smith, J. C.; Kasson, P. M.; van der Spoel, D.; Hess, B.; Lindahl, E. GROMACS 4.5: A High-Throughput and Highly Parallel Open Source Molecular Simulation Toolkit. *Bioinformatics* **2013**, *29*, 845−854.
(27) Bonomi, M.; Branduardi, D.; Bussi, G.; Camilloni, C.; Provasi, D.; Raiteri, P.; Donadio, D.; Marinelli, F.; Pietrucci, F.; Broglia, R. A.; Parrinello, M. PLUMED: A Portable Plugin for Free-Energy Calculations with Molecular Dynamics. *Comput. Phys. Commun.* **2009**, *180*, 1961−1972.
(28) Pertz, O.; Bozic, D.; Koch, A. W.; Fauser, C.; Brancaccio, A.; Engel, J. A New Crystal Structure, Ca^{2+} Dependence and Mutational Analysis Reveal Molecular Details of E-Cadherin Homoassociation. *EMBO J.* **1999**, *18*, 1738−1747.
(29) Bjelkmar, P.; Larsson, P.; Cuendet, M. A.; Hess, B.; Lindahl, E. Implementation of the CHARMM Force Field in GROMACS: Analysis of Protein Stability Effects from Correction Maps, Virtual Interaction Sites, and Water Models. *J. Chem. Theory Comput.* **2010**, *6*, 459−466.
(30) Baştuğ, T.; Kuyucak, S. Energetics of Ion Permeation, Rejection, Binding, and Block in Gramicidin A from Free Energy Simulations. *Biophys. J.* **2006**, *90*, 3941−3950.
(31) Bussi, G.; Donadio, D.; Parrinello, M. Canonical Sampling through Velocity Rescaling. *J. Chem. Phys.* **2007**, *126*, 014101.
(32) Parrinello, M.; Rahman, A. Polymorphic Transitions in Single Crystals: A New Molecular Dynamics Method. *J. Appl. Phys.* **1981**, *52*, 7182.
(33) Tiwary, P.; Parrinello, M. A Time-Independent Free Energy Estimator for Metadynamics. *J. Phys. Chem. B* **2015**, *119*, 736−742.
(34) Juraszek, J.; Saladino, G.; van Erp, T. S.; Gervasio, F. L. Efficient Numerical Reconstruction of Protein Folding Kinetics with Partial Path Sampling and Pathlike Variables. *Phys. Rev. Lett.* **2013**, *110*, 108106.
(35) Bonomi, M.; Barducci, A.; Parrinello, M. Reconstructing the Equilibrium Boltzmann Distribution from Well-Tempered Metadynamics. *J. Comput. Chem.* **2009**, *30*, 1615−1621.
(36) Vendome, J.; Posy, S.; Jin, X.; Bahna, F.; Ahlsen, G.; Shapiro, L.; Honig, B. Molecular Design Principles Underlying β-Strand Swapping in the Adhesive Dimerization of Cadherins. *Nat. Struct. Mol. Biol.* **2011**, *18*, 693−700.
(37) Kozakov, D.; Brenke, R.; Comeau, S. R.; Vajda, S. PIPER: An FFT-Based Protein Docking Program with Pairwise Potentials. *Proteins: Struct., Funct., Bioinf.* **2006**, *65*, 392−406.

DOI: 10.1021/ct5010164
J. Chem. Theory Comput. 2015, 11, 1354−1359